

## Alpha-glucosidase and Alpha-amylase Inhibitors Derived from Naturally Occurring Prenylated Isoflavones

Brandon Hernández-Gutiérrez<sup>1</sup>, María C. Cruz-López<sup>1</sup>, Omar Gómez-García<sup>2</sup>, Elvia Becerra-Martínez<sup>3</sup>, Fabiola E. Jiménez-Montejo<sup>1</sup>, Aarón Mendieta-Moctezuma<sup>1\*</sup>

<sup>1</sup>Centro de Investigación en Biotecnología Aplicada, Instituto Politécnico Nacional, Carretera Estatal Santa Inés Tecuexcomax-Tepetitla, Km 1.5, Tepetitla de Lardizábal, 90700 Tlaxcala, Mexico.

<sup>2</sup>Departamento de Química Orgánica, Escuela Nacional de Ciencias Biológicas, Instituto Politécnico Nacional, Prol. Carpio y Plan de Ayala S/N, 11340 Ciudad de México, Mexico.

<sup>3</sup>Centro de Nanociencias y Micro y Nanotecnologías, Instituto Politécnico Nacional, Av. Luis Enrique Erro S/N, Ciudad de México, 07738, Mexico.

\*Corresponding author: Aarón Mendieta-Moctezuma, email: [amendietam@ipn.mx](mailto:amendietam@ipn.mx)

Received September 3<sup>rd</sup>, 2023; Accepted September 19<sup>th</sup>, 2023.

DOI: <http://dx.doi.org/10.29356/jmcs.v68i1.2129>

**Abstract.** A series of prenylated isoflavones were synthesized to evaluate their inhibitory effect against  $\alpha$ -glucosidase and  $\alpha$ -amylase enzymes, analyzing the bioisosteric effect of the linear or cyclized prenyl moiety in these benzopyran derivatives. Compound **5a** exhibited higher  $\alpha$ -glucosidase inhibition ( $IC_{50} = 60.5 \mu M$ ) and lower  $\alpha$ -amylase inhibition ( $IC_{50} = 85.0 \mu M$ ) compared to acarbose ( $IC_{50} = 527.5 \mu M$  for  $\alpha$ -glucosidase and  $20.1 \mu M$  for  $\alpha$ -amylase). In contrast, prenylated isoflavone **5c** showed higher inhibition in both enzymes ( $IC_{50} = 17.6 \mu M$  for  $\alpha$ -glucosidase and  $21.2 \mu M$  for  $\alpha$ -amylase). This suggests that the attachment of a prenyl moiety to the 7-hydroxy group of isoflavone provides higher inhibition in the enzymes  $\alpha$ -glucosidase and  $\alpha$ -amylase. Docking studies of compounds **5a** and **5c** displayed key interactions towards both enzymes. The type of inhibition for **5c** was analyzed, where the results indicate a competitive inhibition of both  $\alpha$ -glucosidase and  $\alpha$ -amylase. Finally, ADMET studies support that compounds **5a** and **5c** are candidates for the design of novel isoflavones derivatives with antidiabetic potential.

**Keywords:** Diabetes mellitus;  $\alpha$ -glucosidase;  $\alpha$ -amylase; prenylated isoflavones; pyranisoflavones.

**Resumen.** Una serie de isoflavonas preniladas se sintetizaron para evaluar su efecto inhibidor sobre las enzimas  $\alpha$ -glucosidasa y  $\alpha$ -amilasa, analizando el efecto bioisotérico del fragmento prenilo tipo lineal o ciclado en estos benzopiranos derivados. El compuesto **5a** exhibió una inhibición alta de  $\alpha$ -glucosidasa ( $CI_{50} = 60.5 \mu M$ ) y una inhibición más baja de  $\alpha$ -amilasa ( $CI_{50} = 85.0 \mu M$ , respectivamente) en comparación con acarbosa ( $CI_{50} = 527.5$  y  $20.1 \mu M$ ). La isoflavona prenilada **5c** mostró mayor inhibición en ambas enzimas ( $CI_{50} = 17.7 \mu M$  para  $\alpha$ -glucosidasa y  $21.2 \mu M$  para  $\alpha$ -amilasa). Esto sugiere que la unión del fragmento prenilo al hidroxilo de la posición 7 de la isoflavona ocasiona una mayor inhibición en las enzimas  $\alpha$ -glucosidasa y  $\alpha$ -amilasa. Los compuestos **5a** y **5c** mostraron interacciones clave hacia el sitio activo de ambas enzimas, de acuerdo con los cálculos de acoplamiento. Se analizó el tipo de inhibición para **5c**, donde los resultados indican una inhibición competitiva tanto de  $\alpha$ -glucosidasa como de  $\alpha$ -amilasa. Finalmente, los estudios ADMET respaldan que los compuestos **5a** and **5c** son candidatos para el diseño de nuevos derivados de isoflavonas con potencial antidiabético.

**Palabras clave:** Diabetes mellitus;  $\alpha$ -glucosidasa;  $\alpha$ -amilasa; isoflavonas preniladas; piranoisoflavonas.

## Introduction

Type 2 diabetes is characterized by a postprandial increase in blood glucose due to the lack of insulin action or secretion, leading to an increased risk of cardiovascular and cerebrovascular diseases, retinopathy, and cancer. According to the World Health Organization (WHO), about 422 million people have diabetes [1]. A therapeutic treatment of diabetes is to reduce blood glucose levels through enzyme inhibitors. The  $\alpha$ -amylase and  $\alpha$ -glucosidase enzymes are involved in the breakdown of dietary starch and sugars into glucose, where  $\alpha$ -amylase catalyzes the hydrolysis of starch and other carbohydrate polymers through the cleavage of 1-4- $\alpha$ -D-glycosidic links generating smaller oligosaccharides while  $\alpha$ -glucosidase catalyzes the cleavage of the 1-4- $\alpha$ -D-glycosidic bonds of these oligosaccharides into glucose units [2]. Acarbose is a pseudo-tetrasaccharide that inhibits both enzymes, thus delaying glucose absorption and reducing postprandial glucose levels [3]. However, its gastrointestinal side effects have led to the search for new glucosidase inhibitors from diverse sources, such as natural products and synthetic compounds.

Isoflavones are secondary metabolites of plants, these heterocycles are based on a 3-phenylchroman skeleton, biogenetically derived from a 2-phenylchroman skeleton of flavonoid. They are well-known for their beneficial properties mainly exerting antioxidant [4], antidiabetic [5], anticancer [6], anti-inflammatory [7], anti-ulcer [8], and anti-obesity effects [9]. The main isoflavones sources are soybeans and red clover, with daidzein, genistein, and formononetin as the main compounds. These have attracted attention due to their antidiabetic properties, as they reduce blood glucose levels by acting as  $\alpha$ -glucosidase inhibitors [5,10]. Moreover, these natural inhibitors have been employed as lead compounds to obtain new molecules with a higher inhibitory effect on  $\alpha$ -glucosidase as well as low adverse effects [7,9,11,12].

Prenylated isoflavones along with pyranisoflavones are a subclass of natural isoflavones that own at least one prenylated side chain on the flavonoid backbone, exhibiting antimicrobial [13], antidiabetic [14,15], anti-inflammatory [7,16], anticancer [17,18], and neuroprotective properties [12]. Their antidiabetic features are attributed to inhibition of  $\alpha$ -glucosidase enzyme [4,14,19,20]. Structure-activity relationship studies of natural isoflavones as  $\alpha$ -glucosidase and  $\alpha$ -amylase inhibitors suggest that at the C-7 position in the isoflavone core, the presence of a linear or cyclized prenyl moiety seems to favor this effect biological [2,14,20].

The  $\alpha$ -glucosidase and  $\alpha$ -amylase inhibitory activities shown by the isoflavones daidzein, genistein, and their prenylated derivatives have been reported, but no data are available for prenylated formononetin derivatives (calopogonium isoflavone A, 6-methoxycalopogonium isoflavone and maxima isoflavone J), which is important for the development of dual inhibitors on those carbohydrate-hydrolyzing enzymes (Fig. 1) [11,21]. Considering these facts, the aim of the current study was to synthesize prenylated isoflavones derived-formononetin and test their potential as  $\alpha$ -amylase and  $\alpha$ -glucosidase inhibitors. Enzymatic and *in silico* studies were performed to better understand the interaction of the compounds with the active site of both enzymes.

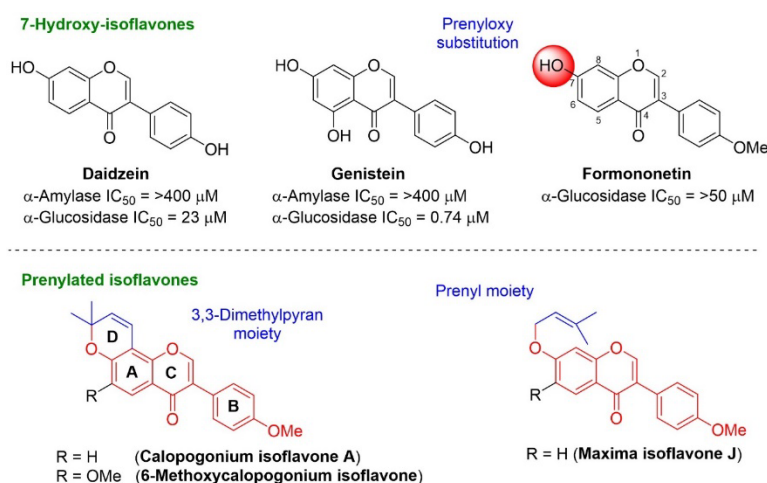


**Fig. 1.** Prenylated isoflavones as potential  $\alpha$ -glucosidase and  $\alpha$ -amylase inhibitors.

## Experimental

### Chemistry

All Raw data measurements of melting points were determined by an Electrothermal apparatus and are uncorrected. Nuclear Magnetic Resonance ( $^1\text{H}$ -,  $^{13}\text{C}$ -NMR) spectra were recorded on Bruker Avance (600 or 750 MHz) spectrometers. The chemical shifts ( $\delta$ ) are expressed in ppm relative to the TMS as internal standard and multiplicities are indicated by the following symbols: s (singlet), d (doublet), t (triplet), dd (double of doublets), brs (broad singlet), brd (broad doublet), and m (multiplet). A UPLC (Waters) coupled to a quadrupole time-of-flight mass spectrometer (Waters Xevo G2-XS QTOF; electrospray ionization mode ESI-tandem quadrupole) was used for UPLC and mass spectrometer analyses (LC-MS/MS). All the reagents used were acquired from Sigma-Aldrich, and anhydrous solvents were obtained by a distillation process. Analytical TLC was carried out on precoated silica gel plates (Merck 60F<sub>254</sub>). Silica gel (230-400 mesh) was used for flash chromatography. The synthesis of compounds **1a-c** and **2a-c** have been previously described [22].

### Method (A) for the preparation of pyranoisoflavones (3a-c)

#### Procedure for the synthesis of 7-hydroxy-isoflavones (2a-c)

A mixture of the corresponding substituted 2,4-dihydroxyacetophenones **1a-c** (1.0 mol equiv.) and DMFDMA (2.0 mol equiv.) was poured into at room temperature in a threaded ACE glass pressure tube with a sealed Teflon screw cap. The mixture was heated at 120 °C for 3 h, diluted with  $\text{CH}_2\text{Cl}_2$  (30 mL) and the solvent was removed under vacuum. The residue was purified by flash chromatography over silica gel (hexane/EtOAc, 80:20).

**7-Hydroxy-3-(4-methoxyphenyl)-4H-chromen-4-one (2a)**. A crystalline beige solid (1.25 g, 92 %). *R<sub>f</sub>* 0.57 (hexane/EtOAc, 7:3); mp 257-258 °C. Characterization of **2a** has been previously reported in the literature [22].

**7-Hydroxy-6-methoxy-3-(4-methoxyphenyl)-4H-chromen-4-one (2b)**. A beige solid (1.25 g, 80 %). *R<sub>f</sub>* 0.15 (hexane/EtOAc, 7:3); mp 222-224 °C. Characterization of **2b** has been previously reported in the literature [22].

**6-Chloro-7-hydroxy-3-(4-methoxyphenyl)-4H-chromen-4-one (2c)**. A beige solid (2.01 g, 82%). *R<sub>f</sub>* 0.27 (hexane/EtOAc, 7:3); mp 232-233 °C. Characterization of **2c** has been previously reported in the literature [22].

#### Procedure for the synthesis of pyranoisoflavones (3a-c)

A solution of the corresponding 7-hydroxy-isoflavones (**2a-c**) (1.0 mol equiv.), 1,1-diethoxy-3-methylbut-2-ene (1.2 mol equiv.), and 3-methylpyridine (0.6 mol equiv.) in xylene (5 mL) was poured into at room temperature in a threaded ACE glass pressure tube with a sealed Teflon screw cap. The mixture was heated at 120 °C for 36 h, diluted with  $\text{CH}_2\text{Cl}_2$  (20 mL) and the solvent was removed under vacuum. The residue was purified by flash chromatography over silica gel (hexane/EtOAc, 90:10)

**3-(4-Methoxyphenyl)-8,8-dimethyl-4H,8H-pyrano[2,3-f]chromen-4-one (3a) [12]**. A white solid (0.10 g, 43 %). *R<sub>f</sub>* 0.55 (hexane/EtOAc, 7:3); m.p. 135-137 °C.  $^1\text{H}$ -NMR (750 MHz,  $\text{CDCl}_3$ )  $\delta$ : 1.50 (s, 6H,  $(\text{CH}_3)_2$ ), 3.84 (s, 3H, OCH<sub>3</sub>), 5.72 (d, *J* = 9.75 Hz, 1H, H-9), 6.81 (d, *J* = 9.75 Hz, 1H, H-10), 6.86 (d, *J* = 9.0 Hz, 1H, H-6), 6.95-6.99 (m, 2H, H-3'), 7.48-7.51 (m, 2H, H-2'), 7.93 (s, 1H, H-2), 8.06 (d, *J* = 8.2 Hz, 1H, H-5).  $^{13}\text{C}$ -NMR (187.5 MHz,  $\text{CDCl}_3$ )  $\delta$ : 28.1 ( $(\text{CH}_3)_2$ ), 55.3 (OCH<sub>3</sub>), 77.6 (C-8), 109.1 (C-10a), 113.9 (C-3'), 114.9 (C-10), 115.1 (C-6), 118.3 (C-4a), 124.2 (C-1'), 124.6 (C-3), 126.7 (C-5), 130.1 (C-2'), 130.2 (C-9), 151.7 (C-2), 152.3 (C-1a), 157.2 (C-6a), 159.5 (C-4'), 175.8 (C=O). HRMS (ESI)  $[\text{M}-\text{H}]^-$  Calculated for:  $\text{C}_{21}\text{H}_{17}\text{O}_4$ . 333.1127. Found: 333.1120  $[\text{M}-\text{H}]^-$ .

**6-Methoxy-3-(4-methoxyphenyl)-8,8-dimethyl-4H,8H-pyrano[2,3-f]chromen-4-one (3b) [23].** A white solid (0.074 g, 61 %). *Rf* 0.33 (hexane/EtOAc, 7:3); m.p. 164-165 °C. <sup>1</sup>H-NMR (750 MHz, CDCl<sub>3</sub>) δ: 1.56 (s, 6H, (CH<sub>3</sub>)<sub>2</sub>), 3.84 (s, 3H, OCH<sub>3</sub>-C-4'), 3.96 (s, 3H, OCH<sub>3</sub>-C-6), 5.74 (d, *J* = 9.75 Hz, 1H, H-9), 6.81 (d, *J* = 9.75 Hz, 1H, H-10), 6.96-6.99 (m, 2H, H-3'), 7.49-7.52 (m, 2H, H-2'), 7.56 (s, 1H, H-5), 7.95 (s, 1H, H-2). <sup>13</sup>C-NMR (187.5 MHz, CDCl<sub>3</sub>) δ: 27.9 ((CH<sub>3</sub>)<sub>2</sub>), 55.3 (OCH<sub>3</sub>-C-4'), 56.3 (OCH<sub>3</sub>-C-6), 78.1 (C-8), 105.1 (C-5), 110.1 (C-10a), 113.9 (C-3'), 115.1 (C-10), 117.6 (C-4a), 124.1 (C-3), 124.4 (C-1'), 130.1 (C-2'), 130.3 (C-9), 147.10 (C-6), 147.16 (C-1a), 147.35 (C-6a), 151.5 (C-2), 159.4 (C-4'), 175.5 (C=O). HRMS (ESI) [M-H]<sup>-</sup> Calculated for: C<sub>22</sub>H<sub>19</sub>O<sub>5</sub>. 363.1232. Found: 363.1225 [M-H]<sup>-</sup>.

**6-Chloro-3-(4-methoxyphenyl)-8,8-dimethyl-4H,8H-pyrano[2,3-f]chromen-4-one (3c).** A white solid (0.09 g, 53 %). *Rf* 0.50 (hexane/EtOAc, 7:3); m.p. 150-151 °C. <sup>1</sup>H-NMR (750 MHz, CDCl<sub>3</sub>) δ: 1.55 (s, 6H, (CH<sub>3</sub>)<sub>2</sub>), 3.83 (s, 3H, OCH<sub>3</sub>), 5.78 (d, *J* = 9.75 Hz, 1H, H-9), 6.80 (d, *J* = 9.75 Hz, 1H, H-10), 6.95-6.99 (m, 2H, H-3'), 7.45-7.50 (m, 2H, H-2'), 7.93 (s, 1H, H-2), 8.12 (s, 1H, H-5). <sup>13</sup>C-NMR (187.5 MHz, CDCl<sub>3</sub>) δ: 28.0 ((CH<sub>3</sub>)<sub>2</sub>), 55.3 (OCH<sub>3</sub>), 79.0 (C-8), 110.7 (C-10a), 113.9 (C-3'), 114.7 (C-10), 118.4 (C-6), 120.4 (C-4a), 123.8 (C-1'), 124.6 (C-3), 126.0 (C-5), 130.0 (C-2'), 130.8 (C-9), 150.5 (C-1a), 151.8 (C-2), 152.6 (C-6a), 159.6 (C-4'), 174.9 (C=O). HRMS (ESI) [M-H]<sup>-</sup> Calculated for: C<sub>21</sub>H<sub>16</sub>ClO<sub>4</sub>. 367.0737. Found: 367.1691.

### Method (B) for the preparation of pyranoisoflavones (3a-c)

#### Procedure for the synthesis of chromenes (4a-c)

Following the method of preparation for **3a**, a mixture of the corresponding 2,4-dihydroxyacetophenone (**1a-c**) (1.0 mol equiv.), 1,1-diethoxy-3-methylbut-2-ene (1.2 mol equiv.), and 3-methylpyridine (0.6 mol equiv.) in xylene (3 mL) was heated at 120 °C for 12 h. The residue was purified by flash chromatography over silica gel (hexane/EtOAc, 98:2).

**1-(5-hydroxy-2,2-dimethyl-2H-chromen-6-yl)-2-(4-methoxyphenyl)ethan-1-one (4a) [24].** Yellow crystals (0.178 g, 71 %). *Rf* 0.63 (hexane/EtOAc, 8:2); m.p. 115-116 °C. <sup>1</sup>H-NMR (750 MHz, CDCl<sub>3</sub>) δ: 1.37 (s, 6H, (CH<sub>3</sub>)<sub>2</sub>), 3.71 (s, 3H, OCH<sub>3</sub>), 4.06 (s, 2H, CH<sub>2</sub>-H-2'), 5.49 (d, *J* = 10.2 Hz, 1H, H-3), 6.26 (d, *J* = 9.0 Hz, 1H, H-8), 6.62 (d, *J* = 10.2 Hz, 1H, H-4), 6.77-6.83 (m, 2H, H-3''), 7.07-7.13 (m, 2H, H-2''), 7.56 (d, *J* = 9.0 Hz, 1H, H-7), 12.88 (s, 1H, OH). <sup>13</sup>C-NMR (187.5 MHz, CDCl<sub>3</sub>) δ: 28.3 ((CH<sub>3</sub>)<sub>2</sub>), 43.8 (CH<sub>2</sub>-C-2'), 55.2 (OCH<sub>3</sub>), 77.7 (C-2'), 108.3 (C-8), 109.3 (C-4a), 112.9 (C-6), 114.1 (C-3''), 115.6 (C-4), 126.3 (C-1''), 128.1 (C-3), 130.3 (C-2''), 131.3 (C-7), 158.5 (C-4''), 159.7 (C-8a), 160.0 (C-5), 202.4 (C=O). HRMS (ESI) [M-H]<sup>-</sup> Calculated for: C<sub>20</sub>H<sub>19</sub>O<sub>4</sub>. 323.1289. Found: 323.1295.

**1-(5-hydroxy-8-methoxy-2,2-dimethyl-2H-chromen-6-yl)-2-(4-methoxyphenyl)ethan-1-one (4b) [25].** Yellow crystals (0.15 g, 65 %). *Rf* 0.44 (hexane/EtOAc, 8:2); m.p. 177-178 °C. <sup>1</sup>H-NMR (750 MHz, CDCl<sub>3</sub>) δ: 1.50 (s, 6H, (CH<sub>3</sub>)<sub>2</sub>), 3.79 (s, 3H, OCH<sub>3</sub>-C-4'), 3.81 (s, 3H, OCH<sub>3</sub>-C-8), 4.13 (s, 2H, CH<sub>2</sub>-H-2'), 5.59 (d, *J* = 9.75 Hz, 1H, H-3), 6.70 (d, *J* = 9.75 Hz, 1H, H-4), 6.86-6.90 (m, 2H, H-3''), 7.15 (s, 1H, H-7), 7.17-7.20 (m, 2H, H-2''), 12.76 (s, 1H, OH). <sup>13</sup>C-NMR (187.5 MHz, CDCl<sub>3</sub>) δ: 28.2 ((CH<sub>3</sub>)<sub>2</sub>), 44.3 (CH<sub>2</sub>-C-2'), 55.2 (OCH<sub>3</sub>-C-4'), 57.0 (OCH<sub>3</sub>-C-8), 78.2 (C-2), 110.4 (C-4a), 111.0 (C-6), 112.9 (C-7), 114.2 (C-3''), 115.9 (C-4), 126.4 (C-1''), 128.3 (C-3), 130.2 (C-2''), 141.1 (C-8), 150.3 (C-8a), 155.5 (C-5), 158.6 (C-4''), 201.9 (C=O). HRMS (ESI) [M-H]<sup>-</sup> Calculated for: C<sub>21</sub>H<sub>21</sub>O<sub>5</sub>. 353.1394. Found: 353.1378.

**1-(8-chloro-5-hydroxy-2,2-dimethyl-2H-chromen-6-yl)-2-(4-methoxyphenyl)ethan-1-one (4c).** A yellow solid (0.143 g, 58 %). *Rf* 0.66 (hexane/EtOAc, 8:2); m.p. 140-142 °C. <sup>1</sup>H-NMR (750 MHz, CDCl<sub>3</sub>) δ: 1.49 (s, 6H, (CH<sub>3</sub>)<sub>2</sub>), 3.79 (s, 3H, OCH<sub>3</sub>-C-4'), 4.12 (s, 2H, CH<sub>2</sub>-H-2'), 5.61 (d, *J* = 9.75 Hz, 1H, H-3), 6.68 (d, *J* = 9.75 Hz, 1H, H-4), 6.86-6.90 (m, 2H, H-3''), 7.14-7.19 (m, 2H, H-2''), 7.70 (s, 1H, H-7), 12.75 (s, 1H, OH). <sup>13</sup>C-NMR (187.5 MHz, CDCl<sub>3</sub>) δ: 28.3 ((CH<sub>3</sub>)<sub>2</sub>), 43.8 (CH<sub>2</sub>-C-2'), 55.2 (OCH<sub>3</sub>-C-4'), 79.1 (C-2), 110.8 (C-4a), 112.3 (C-8), 113.1 (C-6), 114.2 (C-3''), 115.5 (C-4), 125.7 (C-1''), 128.6 (C-3), 130.3 (C-2''), 130.5 (C-7), 155.0 (C-8a), 158.3 (C-5), 158.7 (C-4''), 202.0 (C=O). HRMS (ESI) [M-H]<sup>-</sup> Calculated for: C<sub>20</sub>H<sub>18</sub>ClO<sub>4</sub>. 357.0899. Found: 357.0861.

**Procedure for the synthesis of pyranoisoflavones (3a-c).** Following the method for preparation for **2a**, a mixture of the corresponding chromene (**4a-c**) (1.0 mol equiv.) and DMFDMA (2.0 mol equiv.) was heated at 120 °C for 12 h. The residue was purified by flash chromatography over silica gel (hexane/EtOAc, 90:10).

**3-(4-Methoxyphenyl)-8,8-dimethyl-4H,8H-pyrano[2,3-f]chromen-4-one (3a).** A white solid (0.05 g, 50 %), *Rf* 0.55 (hexane/EtOAc, 7:3); m.p. 135-137 °C.

**6-Methoxy-3-(4-methoxyphenyl)-8,8-dimethyl-4H,8H-pyrano[2,3-f]chromen-4-one (3b).** A white solid (0.046 g, 47 %), *Rf* 0.33 (hexane/EtOAc, 7:3); m.p. 164-165 °C.

**6-Chloro-3-(4-methoxyphenyl)-8,8-dimethyl-4H,8H-pyrano[2,3-f]chromen-4-one (3c).** A white solid (0.055 g, 55 %), *Rf* 0.50 (hexane/EtOAc, 7:3); m.p. 150-151 °C.

### General Method for the preparation of 7-O-prenyl-isoflavones (5a-c)

At room temperature (rt), 3,3-dimethylallyl bromide (1.5 mol equiv.) was added dropwise to a solution of 7-hydroxy-isoflavone **2a-c** (1.0 mol equiv.), and K<sub>2</sub>CO<sub>3</sub> (2.0 mol equiv.) in dried acetone (20 mL), then stirred for 15 minutes. The reaction mixture was refluxed at 60 °C for 3 h, filtered, and the solvent removed under vacuum. The crude residue was purified by flash chromatography over silica gel (hexane/EtOAc, 80:20)

**3-(4-Methoxyphenyl)-7-((3-methylbut-2-en-1-yl)oxy)-4H-chromen-4-one (5a) [7].** A white solid (0.434 g, 87 %). *Rf* 0.57 (hexane/EtOAc, 7:3), mp 131-132 °C. <sup>1</sup>H NMR (750 MHz, DMSO-*d*<sub>6</sub>): δ 1.74 (s, 3H, H-4''), 1.76 (s, 3H, H-5''), 3.79 (s, 3H, CH<sub>3</sub>O), 4.68 (sbr, 2H, CH<sub>2</sub>-H-1''), 5.47 (tbr, 1H, CH-H2''), 6.90-7.10 (m, 3H, H-3', H-6), 7.06 (dbr, *J* = 6.7 Hz, 1H, H-8), 7.43-7.60 (m, 2H, H-2'), 8.01 (dbr, *J* = 6.7 Hz 1H, H-5), 8.41 (sbr, 1H, H-2). <sup>13</sup>C NMR (187.5 MHz, DMSO-*d*<sub>6</sub>): δ 18.5 (C-5''), 25.4 (C-4''), 55.1 (OCH<sub>3</sub>), 65.3 (OCH<sub>2</sub>-C1''), 101.2 (C-8), 113.6 (C-3'), 115.2 (C-6), 117.4 (C-4a), 118.9 (C-2''), 123.3 (C-3), 124.0 (C-1'), 126.8 (C-5), 130.0 (C-2'), 138.3 (C-3''), 153.4 (C-2), 157.3 (C-8a), 159.0 (C-4'), 162.8 (C-7), 174.6 (CO-4). HRMS (ESI) [M-H]<sup>-</sup> Calculated for: C<sub>21</sub>H<sub>19</sub>O<sub>4</sub>: 335.1283. Found: 335.1302 [M-H]<sup>-</sup>.

**6-Methoxy-3-(4-methoxyphenyl)-7-((3-methylbut-2-en-1-yl)oxy)-4H-chromen-4-one (5b).** A white solid (0.177 g, 72 %). *Rf* 0.36 (hexane/EtOAc, 7:3), mp 156-157 °C. <sup>1</sup>H NMR (600 MHz, CDCl<sub>3</sub>): δ 1.71 (s, 3H, H-4''), 1.74 (s, 3H, H-5''), 3.76 (s, 3H, CH<sub>3</sub>O-H-4'), 3.89 (s, 3H, CH<sub>3</sub>O-H-6), 4.61 (d, *J* = 6.6 Hz, 2H, CH<sub>2</sub>-H-1''), 5.47 (t, *J* = 6.6 Hz, 1H, CH-H2''), 6.79 (s, 1H, H-8), 6.86-6.92 (m, 2H, H-3'), 7.39-7.46 (m, 2H, H-2'), 7.54 (s, 1H, H-5), 7.85 (s, 1H, H-2). <sup>13</sup>C NMR (150 MHz, CDCl<sub>3</sub>): δ 18.3 (C-5''), 25.8 (C-4''), 55.2 (OCH<sub>3</sub>-C4'), 56.2 (OCH<sub>3</sub>-C6), 66.2 (OCH<sub>2</sub>-C1''), 100.5 (C-8), 104.9 (C-5), 113.9 (C-3'), 117.7 (C-4a), 118.5 (C-2''), 124.3 (C-1'), 124.5 (C-3), 130.1 (C-2'), 139.0 (C-3''), 148.0 (C-6), 151.7 (C-2), 152.1 (C-8a), 153.6 (C-4'), 159.5 (C-7), 175.5 (CO-4). HRMS (ESI) [M-H]<sup>-</sup> Calculated for: C<sub>22</sub>H<sub>21</sub>O<sub>5</sub>: 365.1389. Found: 365.1386.

**6-Chloro-3-(4-methoxyphenyl)-7-((3-methylbut-2-en-1-yl)oxy)-4H-chromen-4-one (5c).** A white solid (0.206 g, 84 %). *Rf* 0.52 (hexane/EtOAc, 7:3), mp 166-167 °C. <sup>1</sup>H NMR (600 MHz, DMSO-*d*<sub>6</sub>): δ 1.76 (s, 3H, H-4''), 1.79 (s, 3H, H-5''), 3.79 (s, 3H, CH<sub>3</sub>O), 4.78 (d, *J* = 6.6 Hz, 2H, CH<sub>2</sub>-H-1''), 5.50 (t, *J* = 6.6 Hz, 1H, CH-H2''), 6.97-7.03 (m, 2H, H-3'), 7.43 (s, 1H, H-8), 7.50-7.57 (m, 2H, H-2'), 8.05 (s, 1H, H-5), 8.49 (s, 1H, H-2). <sup>13</sup>C NMR (150 MHz, DMSO-*d*<sub>6</sub>): δ 18.2 (C-5''), 25.5 (C-4''), 55.1 (OCH<sub>3</sub>), 66.6 (OCH<sub>2</sub>-C1''), 102.4 (C-8), 113.6 (C-3'), 117.6 (C-4a), 118.4 (C-2''), 120.3 (C-3), 123.3 (C-1'), 123.7 (C-6), 125.7 (C-5), 130.0 (C-2'), 139.1 (C-3''), 153.8 (C-2), 155.8 (C-8a), 157.7 (C-7), 159.1 (C-4'), 173.7 (CO-4). HRMS (ESI) [M-H]<sup>-</sup> Calculated for: C<sub>21</sub>H<sub>18</sub>ClO<sub>4</sub>: 369.0894. Found: 369.0909.

### Biological activity

#### Inhibition of α-glucosidase

A reaction was prepared by mixing 20 μL α-glucosidase solution (0.5 unit/mL), 120 μL of 0.1 M phosphate buffer (pH 6.9), and 10 μL of the samples at concentrations from 400 μM to 4.0 μM. The solution

was incubated in a 96-well microplate at 37 °C for 15 min. Then the enzymatic reaction was initiated by adding 20  $\mu\text{L}$  of 5 mM *p*-NPG solution in 0.1 M phosphate buffer (pH 6.9), followed by incubation at 37 °C for 15 min. The reaction was stopped by adding 80  $\mu\text{L}$  of 0.2 M  $\text{Na}_2\text{CO}_3$  and absorbance was read at 405 nm [22]. Acarbose was used as reference control.  $\text{IC}_{50}$  is the concentration that gives 50 %  $\alpha$ -glucosidase inhibition.

### Inhibition of $\alpha$ -amylase

The reaction mixture consisting of 50  $\mu\text{L}$  of 0.1 M phosphate buffer (pH 6.8), 10  $\mu\text{L}$  of  $\alpha$ -amylase solution (5.0 unit/mL), and 20  $\mu\text{L}$  of the sample at various concentrations (from 100  $\mu\text{M}$  to 5.0  $\mu\text{M}$ ) was placed in a 96-well plate and pre-incubated at 37 °C for 15 min, and 20  $\mu\text{L}$  of 1 % soluble starch (0.1 M phosphate buffer, pH 6.8) was then added as a substrate and incubated at 37 °C for 45 min. Finally, 100  $\mu\text{L}$  of 3,5-dinitrosalicylic acid (DNS) was added and heated at 100 °C for 20 min, and absorbance was then read at 540 nm [26]. Acarbose was used as reference control.  $\text{IC}_{50}$  is the concentration that gives 50 %  $\alpha$ -glucosidase inhibition.

### Kinetic study

Kinetic studies were carried out with  $\alpha$ -glucosidase and  $\alpha$ -amylase using a methodology such as that describe in the inhibitory activity assays. The prenylated isoflavone was evaluated at two concentrations according to their  $\text{IC}_{50}$ . Various concentrations of substrates were used for each of the enzymes in the range of 0.5–5.0 mM for *p*-NPG in  $\alpha$ -glucosidase and 0.1–1.0 % for  $\alpha$ -amylase. The type of inhibition for this compound was determined by utilizing double reciprocal plots. Inhibition constants ( $K_i$ ) were calculated from substrate versus reaction rate curves using nonlinear regression of the enzyme inhibition kinetic function [22].

### Docking studies

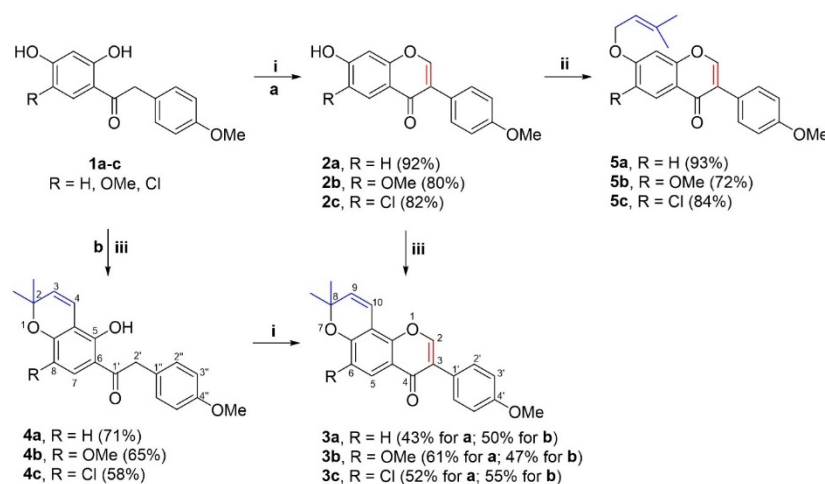
The molecular docking studies were carried out in the AutoDock 4 program [27] using the crystallized proteins of isomaltase from *Saccharomyces cerevisiae* (PDB: 3A4A) and human pancreatic  $\alpha$ -amylase (PDB: 1B2Y) in complex with the inhibitor acarbose. In these proteins, water molecules were removed, hydrogen atoms were added to the polar atoms (considering pH at 7.4), and Kollman charges were assigned with AutoDock Tools 1.5.6. The 3D structures of acarbose (**5**) and isoflavone derivative **5c** were sketched in two dimensions (2D) with ChemSketch and then converted to 3D in a mol2 format using the Open Babel GUI program [28]. The ligands were optimized with PM6 on Gaussian 98 software to obtain the lowest energy conformation. All the possible rotatable bonds, torsion angles, atomic partial charges, and non-polar hydrogens were determined for each ligand. In AutoDockTools, the grid dimensions for  $\alpha$ -glucosidase were  $78 \times 60 \times 78 \text{ \AA}^3$  with points separated by 0.375  $\text{\AA}$  and centered at  $X = 26.313$ ,  $Y = -3.544$ , and  $Z = 26.146$ . The grid dimensions for  $\alpha$ -amylase were  $90 \times 70 \times 66 \text{ \AA}^3$  with points separated by 0.375  $\text{\AA}$  and centered at  $X = 16.758$ ,  $Y = 8.692$ , and  $Z = 49.959$ . The hybrid Lamarckian genetic algorithm was applied for minimization and utilized default parameters. A total of one hundred docking runs were conducted to determine the conformation with the lowest binding energy (kcal/mol), which was adopted for all further simulations. AutoDockTools was used to prepare the script and files as well as to visualize the docking results, and these were edited with Discovery Studio Visualizer [29].

## Results and discussion

### Chemistry

Pyranisoflavones are generally obtained using hydroxyketones as building blocks through two approaches: i) synthesis of hydroxylated isoflavones and formation of the 3,3-dimethyl pyran ring; and ii) synthesis of benzopyran moiety followed by the assembling of the isoflavone core [7]. In order to evaluate the pyran moieties within the isoflavone core, both strategies were applied and the synthesis of prenylated isoflavones is described in scheme 1.

In the first case, 7-hydroxyisoflavones derivatives **2a-c** were prepared in good yields by treatment of 2,4-dihydroxyacetophenones **1a-c** with DMFDMA under thermal conditions [22]. Then, the cyclization of 7-hydroxyisoflavones **2a-c** with 1,1-diethoxy-3-methylbut-2-ene in presence of 3-methylpicoline provided the pyranisoflavones calopogonium isoflavone A (**3a**), 6-methoxycalopogonium isoflavone (**3b**), and 6-chloropyranisoflavone (**3c**) in moderate to good yields. On the other hand, the chromene derivatives **4a-c** were obtained by cyclization of 2,4-dihydroxyketones **1a-c** with 1,1-diethoxy-3-methylbut-2-ene in presence of 3-methylpicoline, which were cyclized with DMFDMA giving the corresponding pyranisoflavones **3a-c**. Finally, the *O*-alkylation reaction of isoflavones **2a-c** with 3,3-dimethylallyl bromide generated the series of 7-prenyloxy-isoflavones **5a-c** in good yields [7].



**Scheme 1.** Synthesis of prenylated isoflavone derivatives. Reagents and conditions: (i) DMFDMA, 120 °C, 3-12 h; (ii) 3,3-dimethylallyl bromide, acetone, K<sub>2</sub>CO<sub>3</sub>, 60 °C, 3 h; (iii) 1,1-diethoxybut-2-ene, 3-methylpicoline, xylene, 120 °C, 24-36 h.

Pyranisoflavones calopogonium isoflavone A (**3a**), 6-methoxycalopogonium isoflavone (**3b**), and 7-prenyloxyisoflavone maxima isoflavone J (**5a**) have been isolated from plants of the genus *Millettia* and *Placolum* (Fabaceae) [23,30-33]. Recently, compound **4b** has been isolated from *P. vietnamense* and has been given the name Placovinone D [25]. The elucidation of the natural and synthetic prenylated isoflavones was confirmed by NMR and HRMS techniques, and the spectroscopic data of **3a-b**, **4b**, and **5a** were in accordance with the published literature [7,12].

### *In vitro* $\alpha$ -glucosidase inhibition

The inhibitory activity of  $\alpha$ -glucosidase was assessed for all the synthesized compounds. The obtained IC<sub>50</sub> values were compared to the corresponding value of acarbose (**6**), a well-known drug that inhibits  $\alpha$ -glucosidase and  $\alpha$ -amylase enzymes. As summarized in Table 1, most of the compounds display significant  $\alpha$ -glucosidase inhibition with IC<sub>50</sub> values in the range of 17.69 to 391.46  $\mu$ M in comparison to **6** with IC<sub>50</sub> of 527.5  $\mu$ M. An exception was compound **3b**, which showed IC<sub>50</sub> >400  $\mu$ M. 7-hydroxyisoflavones **2a-c** showed good inhibitory activity whereas compound **2c** (IC<sub>50</sub> = 91.99  $\pm$  0.21  $\mu$ M) produced a better effect of almost 6-fold higher than **6**. The addition of a cyclized prenyl moiety at C-7 - C-8 (E-ring) of the 7-hydroxyisoflavone backbone led to a significant loss of inhibitory effect with IC<sub>50</sub> values of 208.0  $\pm$  0.45 and 260.1  $\pm$  0.52  $\mu$ M (compounds **3a** and **3c**). Interestingly, chromene benzyl derivatives **4a-c** (without C-ring) displayed greater inhibition than **3a-c**, where **4c** exhibited 9-fold higher than **6**. In order to explore that linear prenyl moiety favors inhibition, derivatives **5a-c** were evaluated. These latter compounds exhibited better inhibitory effect than

pyranoisoflavones (**3a-c**), being **5c** as the most potent derivative ( $IC_{50} = 17.7 \pm 0.02 \mu\text{M}$ ), with almost 30-fold greater inhibition of  $\alpha$ -glucosidase than **6**.

Regarding the inhibitory effect of the cyclized prenyl moiety (D-ring) on the 7-hydroxyisoflavone core, the analysis of the structure-activity relationship revealed that the dimethylpyran group in the pyranoisoflavone (**3a-c**) presented a weak inhibitory behavior. In contrast, chromene benzyl derivatives **4a-c**, compounds without the pyran ring (C-ring) exhibited greater inhibition, which indicates that the hydroxy group contributed to a higher inhibitory effect. These data suggest that the incorporation of a cyclized prenyl moiety to the isoflavone core significantly decreased the  $\alpha$ -glucosidase inhibition, while a prenyloxy moiety at C-7 enhanced inhibitory activity. Furthermore, the presence of the chlorine atom at C-6 increased the inhibitory effects, while that the methoxy group decreased the activity. These results are in accordance with Jo *et al.* who reported that the  $\alpha$ -glucosidase inhibitory activity was stronger in isoflavones with a linear prenyl group than cyclized ones [2,14].

**Table 1.**  $\alpha$ -Glucosidase and  $\alpha$ -amylase inhibition by the test compounds.

Compound	$\alpha$ -Glucosidase inhibition		$\alpha$ -Amylase inhibition	
	% (400 $\mu\text{M}$ )	$IC_{50}$ ( $\mu\text{M}$ )	% (100 $\mu\text{M}$ )	$IC_{50}$ ( $\mu\text{M}$ )
<b>2a</b>	94.21 $\pm$ 0.91	95.78 $\pm$ 0.04 <sup>F</sup>	63.53 $\pm$ 2.55	70.68 $\pm$ 1.2 <sup>D</sup>
<b>2b</b>	92.0 $\pm$ 0.15	111.4 $\pm$ 0.23 <sup>F</sup>	30.69 $\pm$ 2.65	>100
<b>2c</b>	99.65 $\pm$ 0.26	91.99 $\pm$ 0.21 <sup>FG</sup>	81.93 $\pm$ 1.37	56.87 $\pm$ 0.7 <sup>E</sup>
<b>3a</b>	59.34 $\pm$ 1.01	208.0 $\pm$ 0.45 <sup>D</sup>	92.56 $\pm$ 3.70	42.23 $\pm$ 0.9 <sup>F</sup>
<b>3b</b>	32.59 $\pm$ 0.52	>400	6.45 $\pm$ 1.25	- <sup>a</sup>
<b>3c</b>	93.30 $\pm$ 0.61	260.1 $\pm$ 0.52 <sup>C</sup>	99.05 $\pm$ 0.51	34.96 $\pm$ 1.18 <sup>F</sup>
<b>4a</b>	99.38 $\pm$ 0.05	78.01 $\pm$ 0.21 <sup>H</sup>	99.44 $\pm$ 0.17	123.20 $\pm$ 0.03 <sup>C</sup>
<b>4b</b>	94.83 $\pm$ 0.15	147.65 $\pm$ 0.15 <sup>B</sup>	8.69 $\pm$ 0.04	-
<b>4c</b>	99.64 $\pm$ 0.03	57.30 $\pm$ 0.05 <sup>I</sup>	70.61 $\pm$ 0.22	143.10 $\pm$ 0.07 <sup>G</sup>
<b>5a</b>	97.00 $\pm$ 1.65	60.56 $\pm$ 0.14 <sup>GH</sup>	99.33 $\pm$ 0.93	85.09 $\pm$ 1.7 <sup>B</sup>
<b>5b</b>	51.74 $\pm$ 1.67	391.46 $\pm$ 0.18 <sup>E</sup>	6.81 $\pm$ 2.43	-
<b>5c</b>	99.15 $\pm$ 0.30	17.69 $\pm$ 0.02 <sup>H</sup>	98.33 $\pm$ 0.07	21.2 $\pm$ 0.1 <sup>A</sup>
<b>Acarbose</b>	45.65 $\pm$ 1.0	527.5 $\pm$ 0.6 <sup>A</sup>	98.01 $\pm$ 0.25	20.18 $\pm$ 1.48 <sup>G</sup>

Data represent the mean + standard deviation ( $n = 4$ ). Means in a column not sharing the same letter are significantly different at  $p < 0.5$  probability according to Tukey tests; <sup>a</sup> Not active (less than 30% inhibition at 400  $\mu\text{M}$ ).

### In vitro $\alpha$ -amylase inhibition

All the synthesized compounds were assessed for their inhibition of  $\alpha$ -amylase. The  $IC_{50}$  values obtained were compared to the corresponding value of acarbose (**6**) (Table 1). In general, almost all compounds showed good to weak  $\alpha$ -amylase activity with  $IC_{50}$  values in the range of 21.2 to 143.1  $\mu\text{M}$  compared to **6** ( $IC_{50} = 20.18 \pm 1.48 \mu\text{M}$ ). Derivatives **2b**, **3b**, **4b**, and **5b** did not show activity at 100  $\mu\text{M}$ . Initially, 7-hydroxyisoflavones **2a** and **2c** showed moderate to weak inhibitory effects. The incorporation of the 3,3-dimethylpyrano group (D-ring) to the isoflavone core displayed almost two-fold greater effect than their parent compounds **2a** and **2c**. Contrarily, derivatives **4a** and **4c** were the less effective compounds, presenting  $IC_{50}$  values of 123.2  $\pm$  0.03 and 143.1  $\pm$  0.07  $\mu\text{M}$ , respectively. In addition, the presence of the prenyloxy group at C-7 (compound **5a**) resulted in a lower inhibitory effect compared to **2a**. Interestingly, compound **5c** ( $IC_{50} = 21.2 \pm 0.1 \mu\text{M}$ )

significantly increased the inhibitory effect concerning **2c**. Therefore, the presence of a chlorine atom at C-6 of the isoflavone core significantly enhanced the inhibition, while with the methoxy group did not show any inhibitory activity. These observations suggest that by introducing a linear or cyclized prenyl moiety into the isoflavone core, the inhibitory effect of  $\alpha$ -amylase was enhanced.

In summary, the incorporation of a cyclized prenyl moiety (**3a** and **3c**) at the isoflavone scaffold exhibited moderate inhibition of  $\alpha$ -glucosidase and  $\alpha$ -amylase, while that compounds **4a** and **4c** (without C-ring) displayed higher inhibition of  $\alpha$ -glucosidase and lowest inhibition of  $\alpha$ -amylase. On the other hand, a greater inhibition of  $\alpha$ -glucosidase with a moderate inhibition of  $\alpha$ -amylase were found by addition of a prenyloxy moiety (**5a** and **5c**).

### Enzymatic kinetic study

In order to explore the mechanism of interaction of **5c** with  $\alpha$ -glucosidase and  $\alpha$ -amylase, the type of inhibition was evaluated by analyzing Lineweaver-Burk (double reciprocal) plots. The X-axis values represent the reciprocal for the  $\alpha$ -glucosidase substrate, *p*-nitrophenyl- $\alpha$ -D-glucopyranoside (*p*-NPG), thus being  $1/(p\text{-NPG})$ , while for the  $\alpha$ -amylase substrate, starch. Thus being  $1/(\text{starch})$ . The Y-axis value are the reciprocal of the reaction velocity ( $V_o$ ), thus being  $1/V_o$ . Given that the plots intersect the Y-axis, the inhibition for  $\alpha$ -glucosidase exerted by this compound is carried out in competitive mode (Fig. 2(a) and 2(b)). The  $K_i$  value of **5c** is 28.5  $\mu\text{M}$ . The  $K_i$  value for this compound is less than  $K_m$ , indicating that it has a higher affinity for the enzyme than the substrate used in the assay.

The  $\alpha$ -amylase plot made it possible to determine that **5c** is a competitive type of inhibitor. Its  $K_i$  value (15.2  $\mu\text{M}$ ) indicates that has greater affinity for the enzyme.

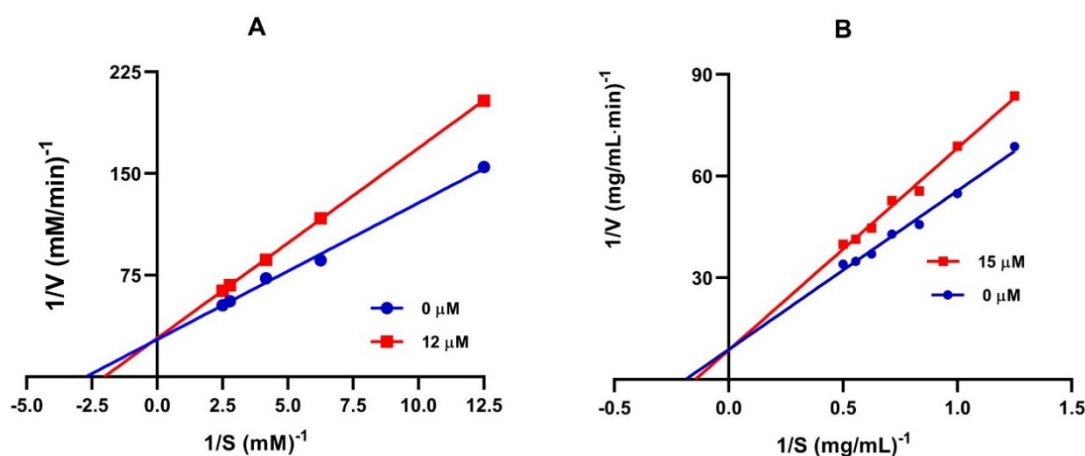


Fig. 2. Lineweaver-Burk plots of **5c** against  $\alpha$ -glucosidase (a) and  $\alpha$ -amylase (b).

### Molecular docking analysis

To explore the binding interactions of the most active compound, molecular docking studies of the isoflavone derivative **5c** and the enzymes isomaltase ( $\alpha$ -glucosidase from *S. cerevisiae*) and the human  $\alpha$ -amylase were carried out. The results are illustrated in 2D and 3D (Fig. 3(a) and 3(b)), revealing that **5c** recognized some of the key amino acid residues in the catalytic pocket, such Arg213, Asp215, Glu277, His351, Asp352, and Arg442 [22,34]. Regarding the binding energy of the compound **5c** with the enzymes, has better binding energy values ( $\Delta G$ ) than the reference drug (**6**) (Table 2). The docking studies with  $\alpha$ -glucosidase reveal that isoflavone system is involved in hydrophobic interactions of various types:  $\pi$ - $\pi$ -T-shaped (Tyr158),  $\pi$ -anion (Asp352),  $\pi$ -cation (Arg442), and  $\pi$ -sigma (Tyr172), as well as hydrogen bond interactions with Asp215 and Asp352. The prenyloxy moiety at C-7 of the isoflavone core shows a hydrophobic interaction with Phe314 and

a hydrophilic interaction with Arg315. According to these results, **5c**, interacts with at least two of the acid residues of the catalytic triad, confirming the competitive inhibition of this compound.

**Table 2.** Docking results of **5c** and acarbose (**6**) at the active site of isomaltase and  $\alpha$ -amylase.

Compound	Binding energy $\Delta G$ (kcal/mol)	Interacting residues	Polar interactions	Hydrophobic interactions
<b>Isomaltase</b>				
<b>6</b>	-7.78	Asp69, Tyr72, His112, Tyr158, Phe159, Phe178, Arg213, Asp215, Val216, Glu277, Gln279, His280, Phe303, Asp307, Arg315, Tyr316, His351, Asp352, Gln353, Glu411, Arg442, Arg446	C-H $\cdots$ O (Asp69) O-H $\cdots$ O (Asp215) O $\cdots$ H-N (Gln279) O-H $\cdots$ O (Asp307) O $\cdots$ H-N (His351) O-H $\cdots$ O (Glu411) O $\cdots$ H-N (Arg446)	-
<b>5c</b>	8.62	Tyr72, Lys156, Ser157, Tyr158, Phe159, Phe178, Arg213, Asp215, Val216, Glu277, Gln279, His280, Phe303, Leu313, Phe314, Arg315, Tyr316, His351, Asp352, Gln353, Glu411, Asn415, Arg442	C-H $\cdots$ O (Asp215) O $\cdots$ H-N (Arg315) C-H $\cdots$ N (His351) C-H $\cdots$ O (Asp352)	$\pi$ -sigma-Tyr172 Alkyl-Lys156 $\pi$ - $\pi$ T-shaped-Tyr158 $\pi$ -alkyl-Phe314, Arg315, Tyr316 $\pi$ -anion-Asp352 $\pi$ -cation-Arg442
<b><math>\alpha</math>-Amylase</b>				
<b>6</b>	-2.92	Asp197, Glu233, Asp300, His305	O-H $\cdots$ O (Asp197) O-H $\cdots$ O (Glu233) C-H $\cdots$ O (Glu233) O-H $\cdots$ O (Asp300) C-H $\cdots$ O (Asp300) O $\cdots$ H-N (His305)	-
<b>5c</b>	-8.25	Trp58, Trp59, Tyr62, Gln63, Gly104, Val107, Thr163, Leu165, Arg195, Asp197, Glu233, His299, Asp300, His305	-	$\pi$ -alkyl-Trp59 $\pi$ - $\pi$ stacked-Trp59, Tyr62 $\pi$ -sigma-Tyr62 Alkyl-Val107, Leu165

For  $\alpha$ -amylase, compound **5c** exhibiting interactions with some amino acid residues at the site binding pocket of the enzyme, including Trp58, Trp59, Tyr62, Leu165, Asp197, Glu233, and Asp300 [33]. Analysis of

docking data showed hydrophobic  $\pi$ - $\pi$  stacked,  $\pi$ -alkyl, and  $\pi$ -sigma interactions with residues Trp59 and Tyr62. The fragment prenyloxy at C-7 of the isoflavone core is involved a hydrophobic interaction of type alkyl (Leu165 and Val107). This analysis shows that **5c** does not interact with the amino acids of the catalytic triad (Asp197, Glu233, and Asp300), suggesting that it is exerting competitive inhibition by interacting at an allosteric site close to the catalytic site.

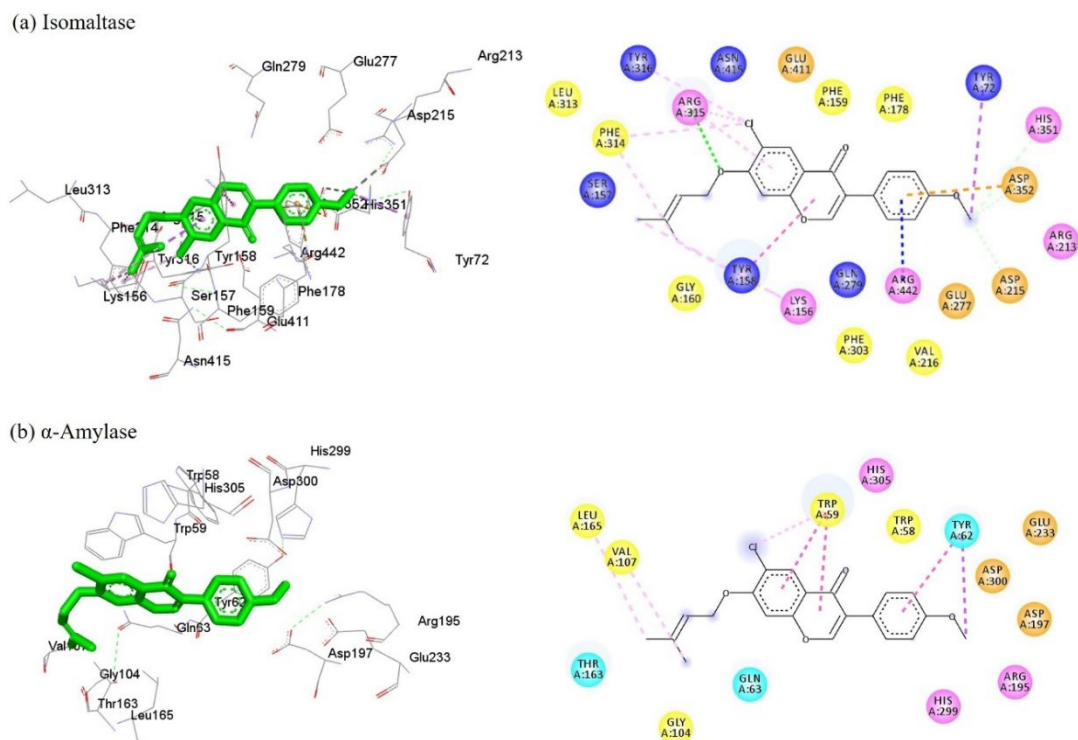


**Fig. 3.** Representation of the interactions of isoflavone **5c** and acarbose at the active site of isomaltase **(a)** and  $\alpha$ -amylase **(b)**. The 3D models illustrate the interactions with the amino acid residues of the catalytic pocket of the enzymes. In the 2D model, conventional hydrogen bond (dark green dotted lines), carbon hydrogen (light green),  $\pi$ -sigma (purple),  $\pi$ - $\pi$  T-shaped and  $\pi$ - $\pi$  stacked (fuchsia),  $\pi$ -alkyl and alkyl (pink),  $\pi$ -anion (orange) and  $\pi$ -cation (blue) interactions are shown. The amino acids are depicted with circles of different colors (pink (basic), orange (acid), cyan (polar), and yellow (non-polar)).

### Lead-likeness, ADME and toxicity prediction

Pharmacokinetics and toxicity predictions of the main  $\alpha$ -glucosidase and  $\alpha$ -amylase inhibitors **3a**, **4a**, **5a**, and **5c** were performed by online software PreADMET and are shown in Table 3 [28]. All title compounds followed Lipinski's Rule of five and showed moderate permeability to Caco-2 cell. Likewise, these compounds have high human intestinal absorption (HIA). Permeability to blood brain barrier (BBB) and skin for all the title compounds is in the acceptable range. Compound **4a** show to be non-mutagenic. Moreover, compounds **4a** and **5c** have not carcinogenic effect on mouse and rat while compounds **3a** and **5a** had carcinogenic effect on rat and did not have this on mouse. Furthermore, cardiotoxicity (hERG inhibition) is of medium risk for all the title compounds.

**Table 3.** Prediction of the lead-likeness and ADMET of compounds **3a**, **4a**, **5a**, **5c**, and acarbose.

Druglikeness/ ADMET <sup>a</sup>	Compound				
	3a	4a	5a	5c	Acarbose
Rule of five <sup>b</sup>	Suitable	Suitable	Suitable	Suitable	Violated
Caco2	39.0976	29.4715	41.3766	53.5303	9.44448
HIA	97.520337	95.737762	97.520337	97.658677	0.000000
BBB	0.0385324	0.342734	0.0776034	0.17198	0.0271005
Skin permeability	-2.5087	-2.03321	-2.62531	-2.6785	-5.17615
Ames test	Mutagen	Non-mutagen	Mutagen	Mutagen	Non-mutagen
Carcino mouse	Negative	Negative	Negative	Negative	Positive
Carcino rat	Positive	Negative	Positive	Negative	Negative
hERG inhibition	Medium risk	Medium risk	Medium risk	Medium risk	Ambiguous

<sup>a</sup>The recommended ranges for Caco2: <25 poor, >500 greater, HIA: >80% is high <25% is poor, BBB = -3.0 to 1.2, and Skin Permeability = -8.0 to -1.

<sup>b</sup>MW molecular weight (<500 g/mol), Log P octanol/water partition coefficient (<5), Log S aqueous solubility, PSA topological polar surface area, HA hydrogen bond acceptor (<10), HD hydrogen bond donor (<5).

## Conclusions

Prenylated isoflavones **3a-c** and **5a-c** were synthesized and their  $\alpha$ -glucosidase and  $\alpha$ -amylase inhibitory activities were evaluated. Compounds **5a** and **5c** showed higher  $\alpha$ -glucosidase activities and moderate  $\alpha$ -amylase activities than standard drug acarbose (**6**). This suggests that bearing a prenyloxy moiety favors the inhibitory effect against  $\alpha$ -glucosidase in comparison to  $\alpha$ -amylase. Enzymatic kinetics showed that **5c** is a competitive inhibitor for both  $\alpha$ -glucosidase and  $\alpha$ -amylase enzymes. Docking studies showed that the hydrophobic effect of the prenyloxy moiety at the C-7 position of the isoflavone backbone favors the interaction with both  $\alpha$ -glucosidase and  $\alpha$ -amylase active sites. Finally, prediction of the lead-likeness and ADMET studies suggest that compounds **5a** and **5c** are candidate for development of dual inhibitors on carbohydrate-hydrolyzing enzymes.

## Acknowledgements

This study was supported by SIP/IPN (SIP20221403, 20231326) and CONACyT (Grants CF-20232-I-2072). BHG gratefully to CONACyT and SIP/IPN (BEIFI) for awarding scholarships. This paper is dedicated to Dr. Joaquín Tamariz Mascarúa with admiration for his academic career in the field of chemistry of natural products.

## References

1. World Health Organization. [Diabetes \(who.int\)](https://www.who.int), accessed in February 2023.
2. Proenca, C.; Ribeiro, D.; Freitas, M.; Fernandes, E. *Crit. Rev. Food Sci. Nut.* **2022**, *62*, 3137-3207. DOI: <https://doi.org/10.1080/10408398.2020.1862755>.

3. Upadhyay, J.; Polyzos, S. A.; Perakakis, N.; Thakkar, B.; Paschou, S. A.; Katsiki, N.; Underwood, P.; Park, K.-H.; Seufert, J.; Kang, E. S.; Sternthal, E.; karagiannis, A.; Mantzoros, C. S. *Metabolism*. **2018**, *78*, 13-42. DOI: <https://doi.org/10.1016/j.metabol.2017.08.10>
4. Jo, Y. H.; Lee, S.; Yeon, S. W.; Ryu, S. H.; Turk, A.; Hwang, B. Y.; Han, Y. K.; Lee, K. Y.; Lee, M. K. *Phytochemistry*. **2022**, *194*, 113016. DOI: <https://doi.org/10.1016/j.phytochem.2021.113016>.
5. Ahmed, Q. U.; Ali, A. H. M.; Mukhtar, S.; Alsharif, M. A.; Parveen, H.; Sabere, A. S. M.; Nawi, M. S. M.; Khatib, A.; Siddiqui, M. J.; Umar, A.; Alhassan, A. M. *Molecules*. **2020**, *25*, 5491. DOI: <https://doi.org/10.3390/molecules25235491>.
6. Hu, W.; Wu, X.; Tang, J.; Zhao, G.; Xiao, N.; Zhang, L.; Li, S. *J. Cell Mol. Med*. **2019**, *23*, 3505-3511. DOI: <https://doi.org/10.1111/jcmm.14248>.
7. Wei, Z.; Yang, Y.; Xie, C.; Li, C.; Wang, G.; Ma, L.; Xiang, M.; Sun, J.; Wei, Y.; Chen, L. *Fitoterapia*. **2014**, *97*, 172-183. DOI: <https://doi.org/10.1016/j.fitote.2014.06.002>.
8. Ndemangou, B.; Sielinou, V. T.; Vardamides, J. C.; Ali, M. S.; Lateef, M.; Iqbal, L.; Afza, N.; Nkengfack, E. *J. Enzyme Inhib. Med. Chem.* **2013**, *28*, 1156-1161. DOI: <https://doi.org/10.3109/14756366.2012.719025>.
9. Cardullo, N.; Muccilli, V.; Pulvirenti, L.; Tringali, C. *J. Nat. Prod.* **2021**, *84*, 654-665. DOI: <https://dx.doi.org/10.1021/acs.jnatprod.0c01387>.
10. Demir, Y.; Durmaz, L.; Taslimi, P.; Gulçin, I. *Biotechnol. Appl. Biochem.* **2019**, 781-786. DOI: <https://doi.org/10.1002/bab.1781>.
11. Sun, H.; Li, Y.; Zhang, X.; Lei, Y.; Ding, W.; Zhao, X.; Wang, H.; Song, X.; Yao, Q.; Zhang, Y.; Ma, Y.; Wang, R.; Zhu, T.; Yu, P. *Bioorg. Med. Chem. Lett.* **2015**, *25*, 4567-4571. DOI: <https://doi.org/10.1016/j.bmcl.2015.08.059>.
12. Wu, C.; Tu, Y.-B.; Li, Z.; Li, Y.-F. *Bioorg. Chem.* **2019**, *88*, 102949. DOI: <https://doi.org/10.1016/j.bioorg.2019.102949>.
13. Polbuppha, I.; Suthiphasilp, V.; Maneerat, T.; Charoensup, R.; Limtharakul, T.; Cheenpracha, S.; Pyne, S. G.; Laphookhieo, S. *Phytochemistry*. **2021**, *187*, 112773. DOI: <https://doi.org/10.1016/j.phytochem.2021.112773>.
14. Jo, Y. H.; Lee, S.; Yeon, S. W.; Turk, A.; Lee, J. H.; Hong, S. M.; Han, Y. K.; Lee, K. Y.; Hwang, B. Y.; Kim, S. Y.; Lee, M. K. *Bioorg. Chem.* **2021**, *114*, 105098. DOI: <https://doi.org/10.1016/j.bioorg.2021.105098>.
15. Lv, H.-W.; Wang, Q.-L.; Luo, M.; Zhu, M.-D.; Lian, H.-M.; Li, W.-J.; Cai, H.; Zhou, Z.-B.; Wang, H.; Tong, S.-Q.; Li, X.-N. *Arch. Pharm. Res.* **2023**, *46*, 207-272. DOI: <http://doi.org/10.1007/s12272-023-01443-4>.
16. Wen, R.; Lv, H.; Jiang, Y.; Tu, P. *Bioorg. Med. Chem. Lett.* **2018**, *28*, 1050-1055. DOI: <https://doi.org/10.1016/j.bmcl.2018.02.026>.
17. Hikita, K.; Salgusa, S.; Takeuchi, Y.; Matsuyama, H.; Nagai, R.; Kato, K.; Murata, T.; Tanaka, H.; Wagh, Y. S.; Asao, N.; Kaneda, N. *Bioorg. Med. Chem.* **2020**, *28*, 115490. DOI: <https://doi.org/10.1016/j.bmc.2020.115490>.
18. Buyinza, D.; Yang, L. J.; Derese, S.; Ndakala, A.; Coghi, P.; Heydenreich, M.; Wong, V. K. W.; Moller, H. M.; Yenesew, A. *Nat. Prod. Res.* **2021**, *35*, 2744-2747. DOI: <https://doi.org/10.1080/14786419.2019.1660335>.
19. Chang, S. K.; Jiang, Y.; Yang, B. *Trends Food Sci. Technol.* **2021**, *108*, 197-213. DOI: <https://doi.org/10.1016/j.tifs.2020.12.022>.
20. Dirir, A.M.; Daou, M.; Yousef, A.; Yousef, L. F. *Phytochem Rev.* **2022**, *21*, 1049-1079. DOI: <https://doi.org/10.1007/s11101-021-09773-1>.
21. Park, M.-H.; Ju, J.-W.; Park, M.-J.; Han, J.-S. *Eur. J. Pharmacol.* **2013**, *712*, 48-52. DOI: <https://doi.org/10.1016/j.ejphar.2013.04.047>.
22. Aguila-Muñoz, D. G.; Cervantes-Espinoza, E.; Escalante, C. H.; Gutiérrez, R. U.; Cruz-López, M. C.; Jiménez-Montejo, F. E.; Villa-Ruano, N.; Gómez-García, O.; Tamariz, J.; Mendieta-Moctezuma, A. *Med. Chem. Res.* **2022**, *31*, 1298-1312. DOI: <https://doi.org/10.1007/s00044-022-02910-1>.

23. Yenesew, A.; Midiwo, J. O.; Waterman, P. G. *J. Nat. Prod.* **1997**, 60, 806-807. DOI: <https://doi.org/10.1021/np9605955>.
24. Yao, H.; Xu, F.; Wang, G.; Xie, S.; Li, W.; Yao, H.; Ma, C.; Zhu, Z.; Xu, J.; Xu, S. *Eur. J. Med. Chem.* **2019**, 167, 485-498. DOI: <https://doi.org/10.1016/j.ejmech.2019.02.014>.
25. Do, L. T. M.; Huynh, T. T. N.; Sichaem, J. *Molecules.* **2022**, 27, 4624. DOI: <https://doi.org/10.3390/molecules27144624>.
26. Chokki, M.; Cudalbeanu, M.; Zongo, C.; Dah-Nouvlessounon, D.; Ghinea, I. O.; Furdui, B.; Raclea, A.; Savadogo, A.; Baba-Moussa, L.; Avamescu, S. M.; Dinica, F. M.; Baba-Moussa, F. *Foods.* **2020**, 9, 434. DOI: <https://doi.org/10.3390/foods9040434>.
27. Morris, G. M.; Huey, R.; Lindstrom, W.; Sanner, M. F.; Belew, R. K.; Goodsell, D. S.; Olson, A. J. *J. Comput. Chem.* **2009**, 30, 2785-2791. DOI: <https://doi.org/10.1002/jcc.21256>.
28. Bioinformatics and Molecular Design Research Center. Seoul, South Korea, 2004. PreADMET Program. Available from: <https://preadmet.webservice.bmdrc.org>, accessed in June 2023.
29. BIOVIA, Dassault Systèmes, Discovery Studio Visualizer v20.1.0.19295, San Diego: Dassault Systèmes (2020).
30. Choudhury, M. K.; Shiferaw, Y.; Sur, K. R.; Dey, D.; Debnathan, S.; Ghosh, S.; Ray, R.; Hazra, B. *J. Coast. Life Med.* **2016**, 4, 556-563. DOI: <https://doi.org/10.12980/jclm.4.2016J6-84>.
31. Deyou, T.; Marco, M.; Heydenreich, M.; Pan, F.; Gruhonjic, A.; Fitzpatrick, P. A.; Koch, A.; Derese, S.; Pelletier, J.; Rissanen, K.; Yenesew, A.; Erdélyi, M. *J. Nat. Prod.* **2017**, 2060-2066. DOI: <https://doi.org/10.1021/acs.jnatprod.7b00255>.
32. Na, Z.; Fan, Q-F.; Song, Q-S.; Hu, H-B. *Phytochem. Lett.* **2017**, 19, 215-219. DOI: <https://doi.org/10.1016/j.phytol.2017.02.002>.
33. Do, L. T. M.; Huynh, T. T. N.; Tran, Q. H. N.; Nguyen, H. T. M.; Nguyen, T. T. A.; Nguyen, T. T. N.; Nguyen, P. H. H.; Sichaem, J. *Nat. Prod. Res.* **2022**, 1-7. DOI: <https://doi.org/10.1080/14786419.2022.2110092>.
34. Aguila-Muñoz, D. G.; Vázquez-Lira, G.; Sarmiento-Tlale, E.; Cruz-López, M. C.; Jiménez-Montejo, F. E.; López y López, V. E.; Escalante, C. H.; Andrade-Pavón, D.; Gómez-García, O.; Tamariz, J.; Mendieta-Moctezuma, A. *Molecules.* **2023**, 28, 4180. DOI: <https://doi.org/10.3390/molecules28104180>.